Kinetics and Catalysis, Vol. 46, No. 1, 2005, pp. 21–28. From Kinetika i Kataliz, Vol. 46, No. 1, 2005, pp. 26–34.
Original English Text Copyright © 2005 by Pyun, Lee, Kim.

Mechanism of the Hydrolysis of N-Aryliminotriphenylphosphoranes[¶]

S.-Y. Pyun[1]*, Y.-H. Lee[2], and T.-R. Kim[3]
[1]*Department of Chemistry, Pukyong National University, Pusan, 608-737, Korea*
** e-mail: sypyun@pknu.ac.kr*
[2]*Department of Chemistry, Wonkwang University, Chunbuk, 570-749, Korea*
[3]*Department of Chemistry, Korea University, 1-Anamdong, Seoul, 136-701, Korea*

Received May 16, 2003

Abstract—Hydrolysis reactions of N-aryliminotriphenylphosphoranes (**I**) at varying pH have been investigated kinetically. The reactions produced aniline derivatives and triphenylphosphine oxide as the products. The reactions are first-order, and the Hammett ρ values are –0.29 and –0.63 at pH 3.0 and 8.0, respectively. The reaction rate increased linearly with acetate ion concentration at $[AcO^-] < 0.05$ M and approached a limiting value at higher base concentration. The plot of $\log k_t$ versus pH shows that there are two different regions in the rate profile; one part in which $\log k_t$ increases with hydronium ion concentration and the other where k_t is a constant regardless of pH. On the basis of these results, a plausible hydrolysis mechanism is proposed. At pH < 8.0, the reaction proceeds by protonation of the iminophosphorane nitrogen atom, followed by the addition of a water molecule. At pH > 8.0, the proton transfer from water to α-nitrogen of the iminophosphorane becomes the rate limiting step.

INTRODUCTION

Iminophosphorane (**A**), alkenephosphorane (**B**), and phosphine oxide (**C**) are among the most important double bonds involving the phosphorus atom [1]. The chemistry of the phosphonium ylide (**B**) has been extensively studied in regard to its synthetic utility [1, 2]. In contrast, relatively little is known about the reactions of the closely related iminophosphoranes (**A**). The literature results indicate that the imino nitrogen of **A** (R = alkyl or aryl) is a typical nucleophile, undergoing reactions such as alkylation, acylation, halogenation, and carbonyl addition [3, 4].

$$\underset{\mathbf{A}}{R_3P = NR'} \quad \underset{\mathbf{B}}{R_3P = CR'_2} \quad \underset{\mathbf{C}}{R_3P = O}$$

Staudinger and coworkers [5] have reported the first isolation of iminophosphoranes formed by reactions of azidobenzene with triphenylphosphine. Briggs *et al.* [6] found that N-aryliminophosphoranes, when treated with alkylhalide in OH^- (aq), afforded the N-alkylbenzeneamine in good yields. Kim [7] has also synthesized N-aryliminotriethoxyphosphoranes and investigated their reactions with benzaldehyde. They reported that iminophosphorane reacts readily with benzaldehyde to form the corresponding imines in good yields. The imine yield increased with the electron withdrawing ability of the substituent of benzaldehyde, although no relationship is readily apparent between the N-aryl substituent of iminophosphorane and the product yields. These results underline the high nucleophilicity of the imino nitrogen of the iminophosphoranes.

In spite of the many uses of iminophosphorane in organic synthesis [8], it has been the subject of only a few kinetic studies [9]. In this work, we have investigated the hydrolysis reaction of N-aryliminotriphenylphosphoranes (**I**) (Eq. (1)). The effects of substituent, general base catalysis, and pH on the rate constant have been studied kinetically. The results of these studies are presented here.

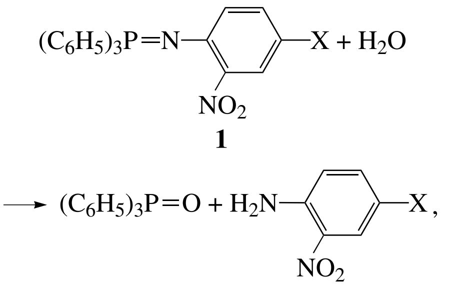

(1)

X = H (**a**), OCH$_3$ (**b**), CH$_3$ (**c**), Cl (**d**), NO$_2$ (**e**).

EXPERIMENTAL

General procedure. All chemicals were reagent grade unless otherwise specified. Substituted azidobenzenes were prepared by the literature method [10]. Kinetic studies were carried out as before [11] using a Pye-Unicam 85000 UV-Vis spectrophotometer 150-20. IR spectra were taken with a Jasco-A-202. ^{1}H NMR

[¶] This article was submitted by the authors in English.

0023-1584/05/4601-0021 © 2005 MAIK “Nauka/Interperiodica”

spectra were obtained with a Varian Model EM-360 (60 MHz), and melting points were measured with a Büchi-510 apparatus. An Orion Research digital-611 Model pH meter was used for pH measurement of the buffer solution. All of the buffer solutions were prepared from reagent grade chemicals, and the ionic strength was maintained at 0.1 M by the addition of sodium chloride except when pH 1.0 and pH > 13.0.

Materials. N-aryliminotriphenylphosphoranes (**1a–1e**) were synthesized as described previously [5]. All of **1a**–**1e** were prepared in reasonable yields by slowly adding the appropriate azidobenzene (25 mmol) in Et_2O (10 ml) to the solution of Ph_3P (25 mmol) in Et_2O (25 ml) at 25°C. The solution was stirred for 2 h, and the solvent was removed under reduced pressure. The products were recrystallized from ethanol. The spectral and analytical data of the compounds were consistent with the proposed structures. The yield (%), melting point (°C), IR (KBr, P=N, cm^{-1}), ^1H NMR ($CDCl_3$), and elemental analysis data for the new compounds are as follows.

$(C_6H_5)_3P{=}NC_6H_4$-2-NO_2 (1a). Yield 87%; m.p. 151–152°C; IR 1381; ^1H NMR δ 7.2 (m, 19H, phenyl). For $C_{24}H_{19}N_2O_2P$ anal. calc.: C, 72.36; H, 4.77; N, 7.03; P, 7.78. Found: C, 72.40; H, 4.75; N, 7.04; P, 7.78.

$(C_6H_5)_3P{=}NC_6H_3$-2-NO_2-4-OCH_3 (1b). Yield 82%; m.p. 136–138°C; IR 1362; ^1H NMR δ 7.1 (m, 18H, phenyl), 3.4 (s, 3H, OCH_3). For $C_{25}H_{21}N_2O_3P$ anal. calc.: C, 70.17; H, 4.95; N, 6.55; P, 7.43. Found: C, 70.11; H, 4.94; N, 6.56; P, 7.40.

$(C_6H_5)_3P{=}NC_6H_3$-2-NO_2-4-CH_3 (1c). Yield 83%; m.p. 139–141°C; IR 1359; ^1H NMR δ 7.1 (m, 18H, phenyl), 2.1 (s, 3H, OCH_3). For $C_{25}H_{21}N_2O_2P$ anal. calc.: C, 72.92; H, 5.15; N, 6.81; P, 7.54. Found: C, 72.88; H, 5.13; N, 6.81; P, 7.64.

$(C_6H_5)_3P{=}NC_6H_3$-2-NO_2-4-Cl (1d). Yield 91%; m.p. 153–155°C; IR 1364; ^1H NMR δ 7.2 (m, 18H, phenyl). For $C_{24}H_{18}ClN_2O_2P$ anal. calc.: C, 66.68; H, 4.20; N, 6.48; P, 7.18. Found: C, 66.83; H, 4.22; N, 6.47; P, 7.12.

$(C_6H_5)_3P{=}NC_6H_3$-2,4-$(NO_2)_2$ (1e). Yield 92%; m.p. 156–158°C; IR 1379; ^1H NMR δ 7.3 (m, 18H, phenyl). For $C_{24}H_{18}N_3O_4P$ anal. calc.: C, 65.11; H, 4.10; N, 9.49; P, 7.01. Found: C, 65.21; H, 4.11; N, 9.48; P, 7.20.

Product studies. The hydrolysis product from the reaction of **1e** under acidic condition was identified by reacting **1e** (7 mmol) with 50 ml HCl solution for 4 h at 80°C. The mixture was extracted with CH_2Cl_2, dried over anhydrous $MgSO_4$, and the solvent was evaporated in a vacuum. The crude product was purified by column chromatography on silica gel using EtOAc/$CHCl_3$ (1:1) as the eluent. The products were 2,4-dinitroaniline and Ph_3PO, which were stable under the experimental conditions. The products were also identified by periodically monitoring the UV absorption of the reaction mixtures under the reaction conditions. The absorbance at 386 nm due to the reactant decreased and those for the 2,4-dinitroaniline (λ_{max} = 340 nm) and Ph_3PO (λ_{max} = 260 nm) increased as the reaction proceeded. Clean isosbestic points were noted at 250 and 350 nm. The reaction product was identified under basic condition by the same procedure as described above for the product analysis under acidic conditions, except that H_3BO_3/NaOH buffer solution (pH = 9.0) was used. The products were 2,4-dinitroaniline and Ph_3PO.

Kinetic studies. A solution of **1a**–**1e** (6.0×10^{-4} M, 1.0 ml) in MeCN was added to a 100 ml volumetric flask and diluted with water to 100.0 ml. The flask was immersed in a water bath maintained at 25°C. Each aliquot portion (3.0 ml) of the solution was removed from the volumetric flask after a measured time interval and was placed in a quartz cuvette. The decrease in absorption at the wavelength of maximum absorption (λ_{max} = 404 nm) for **1a** and its derivatives (**1b**–**1e**, λ_{max} = 386–433 nm) over time was monitored.

pK_a values of iminophosphoranes. The pK_a values of **1a**–**1e** in water were determined by analyzing their absorption spectra by the Davis–Geissman method [12]. The pK_a of iminiumphosphoranes (SH^+) were measured spectrophotometrically at 300–360 and 386–433 nm, where the differences between ε_{SH^+} and ε_S are largest. The pK_a values were determined by plotting of ε_{SH^+} or ε_S vs. pH. The results are summarized in Table 4.

Control experiments. The stability of **1a**–**1e** in MeCN solutions was determined by periodical scanning of the solutions with the UV spectrophotometer. The solutions of **1a**–**1e** in MeCN were stable for at least two weeks when stored in the refrigerator.

RESULTS

Rate constants. Figure 1 shows the plot of log**A** vs. reaction time for the hydrolysis of **1e** at pH 3.5. The plot is linear, indicating that the reaction is first-order to the substrate. Similar results were obtained for all compounds under all reaction conditions employed in this study. The first-order rate constant (k_{obsd}) was calculated from the slope of this plot. The values of k_{obsd} measured at various pH are given in Table 1, from which the pH-rate profile shown in Fig. 2 is constructed. First-order rate constants of the other derivatives are summarized in Table 2.

Substituent effect. The influence of the N-aryl substituent upon the hydrolysis rates of **1a**–**1e** correlated satisfactorily with the Hammett equation using σ values (Fig. 3). The Hammett ρ values are negative at all pH ranges, indicating that electron-donating groups facilitate the reaction. In addition, the value of $\rho = -0.29 \pm 0.06$ at pH 3.0 is smaller than that ($\rho = -0.63 \pm 0.04$) calculated at pH 8.0. This indicates less positive charge development in the transition state under acidic condition.

General base catalysis. To determine whether the reaction is general base catalyzed, the rate constants for **1a** were determined by varying the acetate ion concentration at pH = 4.78. As shown in Fig. 4, the rate increased linearly with the acetate ion concentration at $[AcO^-] < 0.05$ M and reached a limiting value at a higher general base concentration.

Brønsted plot. Table 3 includes the rate constants $(k_1/k_{-1})k_2^B$ for the deprotonation of intermediate **IV** by general bases with different structural types. The $(k_1/k_{-1})k_2^B$ values showed good correlation with the pK_a values of the general bases (Fig. 5). The Brønsted β value is 0.44 ± 0.01 with excellent correlation ($r = 0.997$).

DISCUSSION

The hydrolysis reactions of **1a**–**1e** produced aniline derivatives and triphenylphosphine oxide as the products. The reaction is first-order to the substrate, and the rate increases with hydronium ion concentration at low pH and remains constant at pH > 8.5 (Figs. 1, 2). A reasonable mechanism consistent with these results is shown in schemes 1 and 2.

Under basic conditions, the reaction appears to proceed by the protonation of the α-nitrogen of the P=N bond followed by the addition of a hydroxide ion to β-phosphorus (Scheme 1).

The α-nitrogen of the P=N bond is expected to be basic enough to abstract a proton from water under the reaction conditions, to afford **I**. The addition of water to the latter to produce **II** should be an exothermic process because a new P–O bond is produced. This intermediate would then undergo a rapid intramolecular retro-addition to afford the products. The formation of an intermediate such as **II** has been previously proposed by Jencks in the Schiff base hydrolysis [14]. Although **II** could not be detected experimentally, its half-life was estimated by an indirect kinetic method [15].

Table 1. Rate constants for the hydrolysis of $(C_6H_5)_3P{=}N{-}C_6H_4\text{-}2\text{-}NO_2$ at varying pH and 25°C

pH	Buffer solution**	$k_{obsd} \times 10^6$, s^{-1}	
		obsd.	calc.
1.0	HCl	910	897
2.0	″	898	897
3.0	″	901	892
3.5	HOAc + NaOAc	886	881
4.0	″	832	881
4.5	″	804	764
5.0	″	645	583
5.5	″	446	349
6.0	″	178	177
6.5	$KH_2PO_4 + K_2HPO_4$	89.2	113
7.0	″	45.6	87.4
7.5	″	16.9	22.9
8.0	H_3BO_3 + NaOH	1.02	0.906
9.0	″	0.469	0.512
10.0	″	0.513	0.512
11.0	NaOH	0.508	0.512
12.0	″	0.511	0.512
13.0	″	0.512	0.512
14.0	″	0.512	0.512

* [Substrate] = 6.0×10^{-6} M.

** The ionic strength was maintained at 0.1 M by the addition of sodium chloride except at pH 1.0 and above 13.0. Estimated uncertainty, ±5%.

The rate-limiting step for this reaction may be assessed by the Hammett ρ value. Figure 3 shows that the Hammett ρ value –0.63 at pH 8.0, indicating a small positive charge development at the reaction site in the transition state. Since the electron density at the reac-

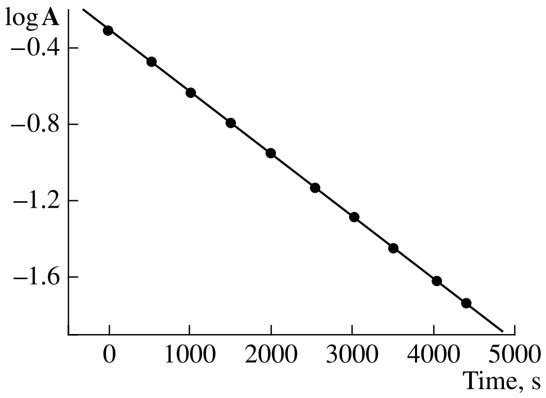

Fig. 1. Plot of log absorbance vs. time for the hydrolysis of $(C_6H_5)_3P{=}N{-}C_6H_3\text{-}2{,}4\text{-}(NO_2)_2$ at pH 3.5 and 25°C.

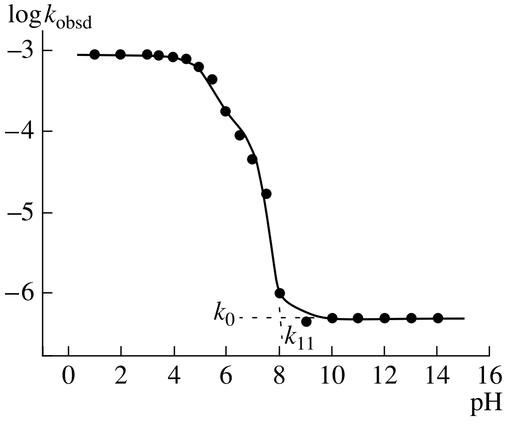

Fig. 2. pH-rate profile for the hydrolysis of $(C_6H_5)_3P{=}N{-}C_6H_4\text{-}2\text{-}NO_2$ at 25°C. Circles are experimental points, and solid line is drawn according to equation (11).

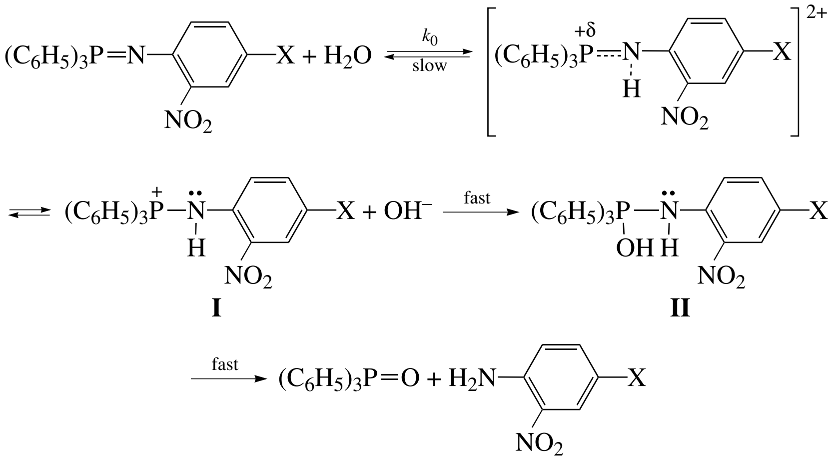

Scheme 1.

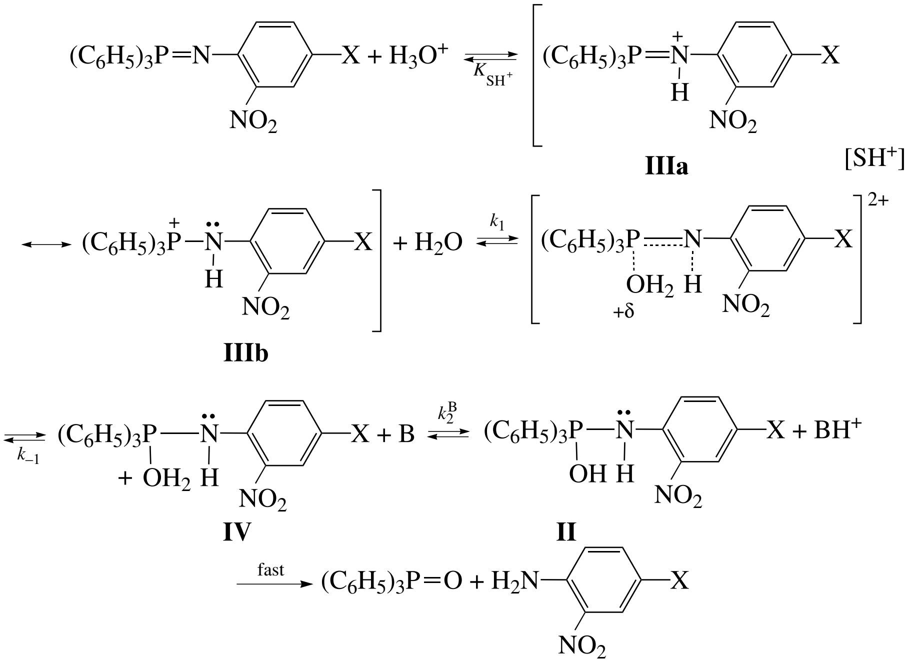

Scheme 2.

tion site decreases in the first step and remains nearly the same in the second step, the small negative ρ value would be consistent if either step is rate limiting. However, considering that deprotonation from **I** would be endothermic, whereas addition of OH^- to **I** should be exothermic (vide supra), it seems most reasonable to expect that the first step is rate limiting.

The plausible mechanism under acidic condition is in Scheme 2, which is similar to that shown in Scheme 1 except that water is added to the SH^+.

In the first step, the α-nitrogen of the P=N bond is assumed to be protonated by H^+ because nitrogen is a stronger base than phosphorus. Resonance stabilization by **IIIb** is important because the positive charge is delocalized over the phosphorus atom. In addition, the resulting protonated iminiumphosphorane (SH^+) species is highly reactive toward nucleophilic attack at the β-phosphorus because of the contribution by **IIIb**. In the second step, either H_2O or OH^- may add to [SH^+]. However, the second possibility has been ruled out because the hydroxide ion concentration is much smaller than that of water. A similar mechanism was proposed by Chaturvedi *et al.* [9a] for the hydrolysis of iminotriethoxyphosphorane. They have also provided strong evidence in support of the existence of intermediate (**IV**).

The rate-determining step of the reaction may be determined by the ρ, β, and general base effect. The ρ value measured at pH 3.0 is –0.29, which is significantly smaller than the ρ = –0.63 at pH 8.0. An electron-donating substituent at the N-aryl ring is expected to increase K_{SH^+} and decrease k_1. This would predict a negative ρ value for the former and a positive value for the latter, respectively. On the other hand, k_2^B should be relatively independent of the aryl substituent because the $-OH_2^+$ is too far away from the substituent, i.e., the ρ value should be near zero. Therefore, the small ρ value could be explained if either k_1 or k_2^B is the rate-determining step. Note that the protonation step is assumed to be rate limiting under basic conditions (vide supra).

Additional evidence in support of this conclusion is provided by the general base catalysis. Figure 4 shows that $\log k_{obsd}$ increases linearly with acetate ion concentration when $[AcO^-] < 0.05$ M. This indicates that the general base catalyzes the deprotonation step and that k_2^B is involved in the rate-limiting step under these conditions. On the other hand, the rate of hydrolysis approaches the limiting values when $[AcO^-] > 0.05$ M. Under this condition, $k_2^B[AcO^-] \gg k_{-1}$, and k_1 becomes the rate-determining step. It is interesting to note that the Brønsted β value for this reaction is 0.44. This indicates a significant proton transfer in the transition state.

The pH-rate profile shown in Fig. 2 provides convincing evidence in support of the proposed mechanism under all reaction conditions. The observed constant (k_{obsd}) can be divided into two parts, each representing a different mechanism:

$$k_{obsd} = k_{11}\left[1 - \frac{K_{SH^+}}{[H_3O^+] + K_{SH^+}}\right] + k_0. \qquad (2)$$

where k_{11} is the rate constant for the addition of water or a hydroxide ion to conjugated acid (SH^+) and k_0 is the rate constant for the hydrolysis reaction which is insensitive to pH, i.e., K_{SH^+} can be defined as the acid dissociation constant of the protonated form, SH^+. $K_{SH^+}/[H_3O^+] + K_{SH^+}$ is the mole fraction of the conjugated acid (SH^+) species at each pH.

The steady-state assumption can be employed frequently, since the concentration of highly reactive intermediates generally attains a low concentration quite rapidly. When assuming the low pH mechanism, one can apply the steady-state approximation with respect to [**IV**] [11].

Table 2. Observed rate constants for the hydrolysis of $(C_6H_5)_3P{=}N{-}C_6H_4\text{-}2\text{-}NO_2\text{-}4\text{-}X$ at varying pH and 25°C

pH	Buffer solution	$k_t \times 10^{-6}$, s^{-1}			
		1b	**1c**	**1d**	**1e**
1.0	HCl	994	957	821	521
2.0	″	993	956	820	512
3.0	″	993	957	778	480
3.5	HOAc + NaOAc	947	952	743	290
4.0	″	932	933	594	126
4.5	″	911	908	402	52.1
5.0	″	862	848	298	36.8
5.5	″	665	633	81.2	7.74
6.0	″	359	309	43.2	1.56
6.5	$KH_2PO_4 + K_2HPO_4$	101	90.2	9.87	0.931
7.0	″	47.2	45.4	4.79	0.733
7.5	″	8.21	11.2	1.13	0.659
8.0	H_3BO_3 + NaOH	1.85	1.40	0.774	0.373
9.0	″	0.821	0.781	0.448	0.370
10.0	″	0.833	0.802	0.434	0.371
11.0	NaOH	0.827	0.785	0.431	0.372
12.0	″	0.826	0.784	0.431	0.371
13.0	″	0.826	0.784	0.431	0.371
14.0	″	0.826	0.784	0.431	0.371

Notes: [Substrate] = 6.0×10^{-6} M.
The ionic strength was maintained at 0.1 M by the addition of sodium chloride except at pH 1.0 and above 13.0. Estimated uncertainty, ±5%.

Table 3. Effect of base strength upon the $(k_1/k_{-1})k_2^B$ values for the hydrolysis of $(C_6H_5)_3P{=}N{-}C_6H_4\text{-}2\text{-}NO_2$ at 25°C

Base	pK_a*	$(k_1/k_{-1})k_2^B$, s^{-1}
H_2O	–1.70	1.06×10^{-3}
$ClCH_2COO^-$	2.82	1.91×10^{-1}
CH_3COO^-	4.75	1.66
p-Toludine	5.18	2.82
Pyridine	5.36	3.31
Lutidine	6.64	1.23×10
$H_2PO_4^-$	7.32	2.09×10
OH^-	15.7	5.32×10^4

* Reference [13].

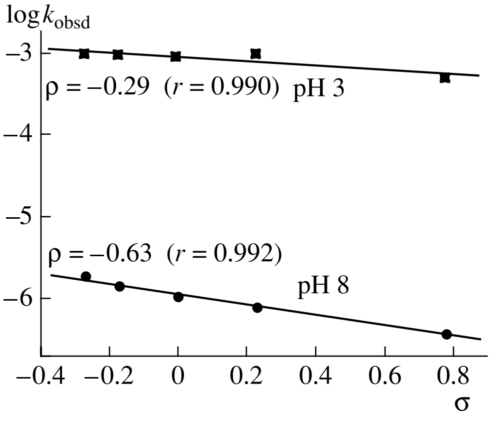

Fig. 3. Hammett plots for the hydrolysis of N-aryliminotriphenylphosphoranes [$(C_6H_5)_3P{=}N{-}C_6H_3\text{-}2\text{-}NO_2\text{-}4\text{-}X$] at pH 3.0, 8.0 and 25°C.

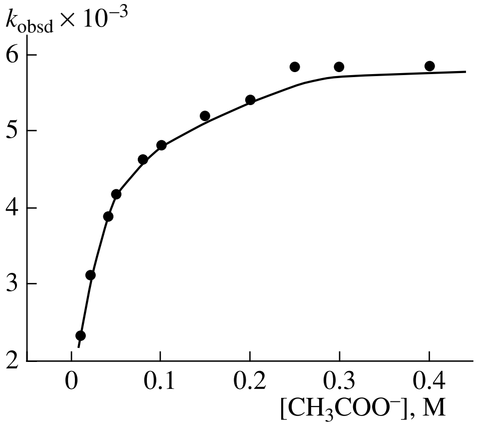

Fig. 4. General base catalysis hydrolysis of $(C_6H_5)_3P{=}N{-}C_6H_4\text{-}2\text{-}NO_2$ at pH 4.78 and 25°C. Circles are experimental points, and solid line is drawn according to Eq. (17c).

The rate equation can be expressed as

$$w = -\frac{[SH^+]}{dt} = k_{11}[SH^+] = \frac{k_1 k_2^B \sum [B]}{k_{-1} + k_2^B \sum [B]}[SH^+], \quad (3)$$

where

$$k_{11} = \frac{k_1 k_2^B \sum [B]}{k_{-1} + k_2^B \sum [B]} \quad (4)$$

or

$$\frac{1}{k_{11}} = \frac{k_{-1} + k_2^B \sum [B]}{k_1 k_2^B \sum [B]} = \frac{1}{k_1} + \frac{1}{\left(\frac{k_1}{k_{-1}}\right) k_2^B \sum [B]}. \quad (5)$$

From Eq. (4), it can shown that, if the concentration of general base is high ($k_2^B[B] \gg k_{-1}$), then $k_{11} = k_1$. Thus, if the concentration of general base is high, k_{11} will take 5.84×10^{-3} s^{-1}, which is the limiting value of general base catalysis in Fig. 4.

If water and hydroxide ion are the only general bases present, Eq. (5) becomes

$$\frac{1}{k_{11}} = \frac{1}{k_1} + \frac{1}{\left(\frac{k_1}{k_{-1}}\right)\{k_2^B[H_2O] + k_2^{OH}[OH^-]\}}. \quad (6)$$

At pH < 3.0, the concentration of hydroxide is negligible, Eq. (6) becomes

$$\frac{1}{k_{11}} = \frac{1}{k_1} + \frac{1}{\left(\frac{k_1}{k_{-1}}\right)\{k_2^{H_2O}[H_2O]\}}. \quad (7)$$

As an example, the overall rate equation (k_{obsd}) for the hydrolysis of **1a** can be determined by the following method. At high general base concentration, k_{11} = 5.84×10^{-3} s^{-1}, which is the limiting value of general base catalysis in Fig. 4. At low pH, since the $k_2^{OH}[OH^-]$ is negligible compared to the $(k_1/k_2)/k_2^{H_2O}$, the value of $(k_1/k_2)/k_2^{H_2O}[H_2O]$ can be determined from $k_1 = 5.84 \times 10^{-3}$ s^{-1}, and the observed rate constant $k_{obsd} = 9.01 \times 10^{-4}$ s^{-1} at pH 1.0 and is found to be 1.06×10^{-3} s^{-1}. In addition, by substituting $k_{obsd} = 1.78 \times 10^{-4}$ s^{-1} at pH 6.0 into Eq. (6), $k_2^{OH} = 5.32 \times 10^4$ s^{-1} can be obtained. This measures the efficiency of hydroxide ion as a base catalyst, **B**, in our mechanism.

Hence, the rate constant k_{11} becomes

$$\frac{1}{k_{11}} = \frac{1}{5.84 \times 10^{-3}} + \frac{1}{1.06 \times 10^{-3} + 5.32 \times 10^4[OH^-]}, \quad (8)$$

$$\frac{1}{k_{11}} = \frac{6.90 \times 10^{-3} + 5.32 \times 10^4[OH^-]}{6.19 \times 10^{-6} + 3.11 \times 10^2[OH^-]}, \quad (9)$$

$$k_{11} = \frac{6.19 \times 10^{-6} + 3.11 \times 10^2[OH^-]}{6.90 \times 10^{-3} + 5.32 \times 10^4[OH^-]}. \quad (10)$$

Based on Fig. 2, we obtained $k_0 = 5.12 \times 10^{-7}$ s^{-1} for pH greater than 8.0. K_{SH^+} of **1a** in water gave 6.03×10^{-6} (Table 4). By substituting the above data into Eq. (2), the overall rate equation constant (k_{obsd}) can be obtained. As a result, the overall rate equation constant becomes

$$k_{obsd} = \frac{6.19 \times 10^{-6} + 3.11 \times 10^2[OH^-]}{6.90 \times 10^{-3} + 5.32 \times 10^4[OH^-]} \times \left[1 - \frac{6.03 \times 10^{-6}}{[H_3O^+] + 6.03 \times 10^{-6}}\right] + 5.12 \times 10^{-7}. \quad (11)$$

Table 1 and Fig. 2 show that the values of overall rate constant k_{obsd} calculated by Eq. (11) are consistent with observed values.

If water, hydroxide ion, and the various bases are present as the general base catalyst, Eq. (6) becomes

$$\frac{1}{k_{11}} = \frac{1}{k_1} + \frac{1}{\left(\frac{k_1}{k_{-1}}\right)\{k_2^{H_2O}[H_2O] + k_2^{OH}[OH^-] + k_2^{B}[B]\}}. \quad (12)$$

From the $k_1 = 5.84 \times 10^{-3}$ s^{-1}, $(k_1/k_{-1})/k_2^{H_2O}[H_2O] = 1.06 \times 10^{-3}$ s^{-1}, $(k_1/k_{-1})k_2^{OH}[OH^-] = 5.32 \times 10^4$ s^{-1} and observed rate constant (k_t), the values of catalytic constants of various bases ($(k_1/k_{-1})k_2^B$) can be determined. The values of the ratio $(k_1/k_{-1})k_2^B$ calculated by Eq. (12) and pK_a of the bases are given in Table 3, and Fig. 5 shows the Brønsted plot. Note that the catalytic constant k_2^B cannot be separated from the hydration equilibrium constant k_1/k_{-1}. However, $(k_1/k_{-1})k_2^B$ will be mainly dependent on k_2^B because the term k_1/k_{-1} is contained in all catalytic constants.

The calculated K_{SH^+} values are summarized in Table 4. As an example, by substituting $k_{obsd} = 1.78 \times 10^{-4}$ s^{-1}, $[OH^-] = 10^{-8}$ M and $[H_3O^+] = 10^{-6}$ M at pH 6.0 into Eq. (11), the results of calculation are consistent with the observed values.

Similarly, the rate equation obtained for the hydrolysis of **1a** derivatives:

p-OCH$_3$:

$$k_{obsd} = \frac{7.86 \times 10^{-6} + 1.56 \times 10^{2}[OH^-]}{7.89 \times 10^{-3} + 2.32 \times 10^{4}[OH^-]} \times \left[1 - \frac{2.24 \times 10^{-6}}{[H_3O^+] + 2.24 \times 10^{-6}}\right] + 8.26 \times 10^{-7}, \quad (13)$$

p-CH$_3$:

$$k_{obsd} = \frac{7.29 \times 10^{-6} + 2.09 \times 10^{2}[OH^-]}{7.63 \times 10^{-3} + 3.21 \times 10^{4}[OH^-]} \times \left[1 - \frac{2.82 \times 10^{-6}}{[H_3O^+] + 2.82 \times 10^{-6}}\right] + 7.84 \times 10^{-7}, \quad (14)$$

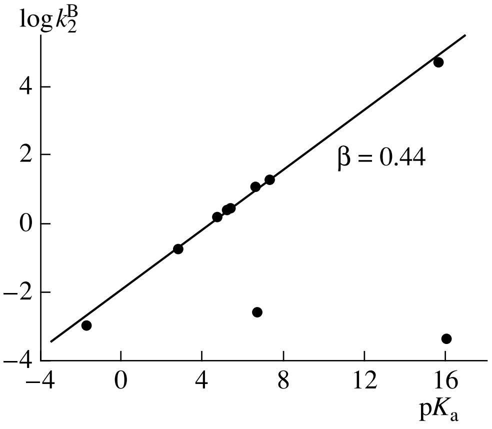

Fig. 5. Brønsted plot for the hydrolysis of $(C_6H_5)_3P{=}N{-}C_6H_4\text{-}2\text{-}NO_2$ promoted by various bases in water at 25°C.

p-Cl:

$$k_{obsd} = \frac{4.24 \times 10^{-6} + 4.75 \times 10^{2}[OH^-]}{5.18 \times 10^{-3} + 1.14 \times 10^{4}[OH^-]} \times \left[1 - \frac{3.72 \times 10^{-5}}{[H_3O^+] + 3.72 \times 10^{-5}}\right] + 4.31 \times 10^{-7}, \quad (15)$$

p-NO$_2$:

$$k_{obsd} = \frac{1.22 \times 10^{-6} + 2.40 \times 10^{4}[OH^-]}{2.34 \times 10^{-3} + 3.05 \times 10^{7}[OH^-]} \times \left[1 - \frac{5.01 \times 10^{-4}}{[H_3O^+] + 5.01 \times 10^{-4}}\right] + 3.71 \times 10^{-7}. \quad (16)$$

If acetate ions are present as a general base catalyst, Eq. (5) becomes

Table 4. pK_a values of N-aryliminotriphenylphosphoranes $[(C_6H_5)_3P{=}N{-}C_6H_4\text{-}2\text{-}NO_2\text{-}4\text{-}X]$ in water

X	pK_a	$K_{SH}^+ \times 10^6$	
		obsd.	calc.
OCH$_3$	5.65	2.24	2.24
CH$_3$	5.55	2.82	2.83
H	5.22	6.03	6.05
Cl	4.43	37.2	37.3
NO$_2$	3.30	501	504

Note: [Substrate] = 3.18×10^{-5} M.

$$\frac{1}{k_{11}} = \frac{1}{k_1} + \frac{1}{\left(\frac{k_1}{k_{-1}}\right)\{k_2^{H_2O}[H_2O] + k_2^{OH}[OH^-] + k_2^{AcO}[AcO^-]\}}. \qquad (17)$$

From the value of $k_1 = 5.84 \times 10^{-3}$ s^{-1}, $(k_1/k_{-1}) \times k_2^{H_2O}[H_2O] = 1.06 \times 10^{-3}$ s^{-1}, $(k_1/k_{-1})k_2^{OH} = 5.32 \times 10^4$ s^{-1}, $[CH_3COO^-] = 0.1$ M, $[OH^-] = 6.03 \times 10^{-10}$ M, and the observed rate constant $k_{obsd} = 4.82 \times 10^{-3}$ s^{-1}, the acetate ion catalytic constant value $(k_1/k_{-1})k_2^{AcO} = 2.42 \times 10^{-4}$ s^{-1} can be obtained. By substituting the above into Eq. (12), k_{11} is given by the following Eq. (17a).

$$\frac{1}{k_{11}} = \frac{7.09 \times 10^{-3} + 2.64 \times 10^{-1}[AcO^-]}{7.19 \times 10^{-6} + 1.54 \times 10^{-3}[AcO^-]}, \qquad (17a)$$

$$k_{11} = \frac{7.19 \times 10^{-6} + 1.54 \times 10^{-3}[AcO^-]}{7.09 \times 10^{-3} + 2.64 \times 10^{-1}[AcO^-]}. \qquad (17b)$$

As a result, the overall rate constant becomes

$$k_{obsd} = \frac{7.19 \times 10^{-6} + 1.54 \times 10^{-3}[AcO^-]}{7.09 \times 10^{-3} + 2.64 \times 10^{-1}[AcO^-]} \times \left[1 - \frac{6.03 \times 10^{-6}}{[H_3O^+] + 6.03 \times 10^{-6}}\right] + 5.12 \times 10^{-7}. \qquad (17c)$$

Figure 4 shows that the values of overall rate constant k_{obsd} calculated by (17c) are in good agreement with the observed values.

ACKNOWLEDGMENTS

This work was supported by Wonkwang University in 2004.

REFERENCES

1. Goldwhite, H., *Introduction to Phosphorus Chemistry*, Cambridge University Presss, U.K., 1981.
2. Trippett, S., *Advances in Organic Chemistry*, Wiley-Interscience, New York, 1960, Vol. 1, p. 83.
3. Johnson, A.W., *Ylide Chemistry, Academic Press*, New York, 1966.
4. Wong, S. C. K. and Johnsow, A. W., *J. Org. Chem.*, 1972, vol. 37, p. 1850.
5. Standinger, H. and Meyer, J., *Helv. Chem. Acta.*, 1919, vol. 3, p. 635.
6. Briggs, E.M., Brown, G.W., Jiricny, J., and Medinine, M.F., *Synthesis*, 1980, vol. 4, p. 2956.
7. Kim, T.R., Cho, B.R., and Lee, Y.H., *Bul. Korean Chem. Soc.*, 1987, vol. 8, p. 48.
8. (a) Molina, P., Alajarin, M., and Argues, A., *Synthesis*, 1982, vol. 6, p. 596. (b) Stuckwisch, C.G., *J. Org. Chem.*, 1976, vol. 41, p. 1173. (c) Vaulx, R.L., Jones, N.F., and Hauser, C.R., *J. Org. Chem.*, 1965, vol. 30, p. 58.
9. (a) Chaturvedi, R.K., Pletcher, T., Zioudlon, C., and Schmir, G.L., *Tetrahedron Lett.*, 1970, p. 4339. (b) Challis, J.A. and Iley, J.N., *J. Chem. Soc.*, Perkin Trans. 2, 1978, p. 813.
10. Smith P. A.S. and Boyer, J.H., *Organic Synthesis*, John-Wiley Sons, Inc. New York, 1960, vol. IV, p. 75.
11. (a) Kim, T.R., Lee, S.Y., Pyun, S.Y., Kim, J.C., and Han, M.S., *Bull. Korean Chem.* Soc., 1999, vol. 20, p. 1213. (b) Kim, T.R., Chang, D.I., and Pyun, S.Y., *J. Korean Chem. Soc.*, 1996, vol. 40, p. 33.
12. Davis, C.T. and Geissman, T.A., *J. Am. Chem. Soc.*, 1954, vol. 76, p. 3057.
13. Kim, T.R. and Huh, T.S., *J. Korean Chem. Soc.*, 1974, vol. 18, p. 430.
14. Jencks, W.P., *J. Am. Chem. Soc.*, 1959, vol. 81, p. 475.
15. (a) Duclos, J.M. and Haake, P., *Biochemistry*, 1974, vol. 113, p. 5358. (b) Zoltewicz, J. and Uray, G., *J. Org. Chem.*, 1980, vol. 45, p. 2104. (c) Kluger, R. and Smith, T., *J. Am. Chem. Soc.*, 1981, vol. 103, p. 884.
16. Leffler, J.E. and Grunwald, E., *Rates and Equilibria of Organic Reactions*, Wiley, New York, 1963. (b) Kresge, A., *J. Acc. Chem. Res.*, 1975, vol. 8, p. 354. (c) Jencks, W.P., *Chem. Rev.*, 1985, vol. 85, p. 511. (d) Jencks, W.P., *Bull. Soc. Chim. Fr.*, 1988, p. 218.